

Article

Efficacy of Column Scatter Plots for Presenting Retinitis Pigmentosa Phenotypes in a Japanese Cohort

Ken Ogino, Akio Oishi, Maho Oishi, Norimoto Gotoh, Satoshi Morooka, Masako Sugahara, Tomoko Hasegawa, Manabu Miyata, and Nagahisa Yoshimura

Department of Ophthalmology and Visual Sciences, Kyoto University Graduate School of Medicine, Kyoto, Japan

Correspondence: Ken Ogino, Department of Ophthalmology and Visual Sciences, Kyoto University Graduate School of Medicine, Sakyo-ku, Kyoto 606-8507, Japan. e-mail: kenboo@kuhp.kyoto-u.ac.jp

Received: 13 October 2015

Accepted: 27 January 2016

Published: 4 March 2016

Keywords: retinitis pigmentosa; genotype-phenotype; Japan; column scatter plot

Citation: Ogino K, Oishi A, Oishi M, et al. Efficacy of column scatter plots for presenting retinitis pigmentosa phenotypes in a Japanese cohort. *Trans Vis Sci Tech.* 2016;5(2):4, doi: 10.1167/tvst.5.2.4

Purpose: We evaluated the efficacy of column scatter plots to describe genotype-phenotype correlations in a Japanese cohort with retinitis pigmentosa (RP).

Methods: Clinical records of 121 patients with RP with identified causative mutations were reviewed. Visual acuity, central and peripheral visual fields, electroretinography (ERG), lens status, and measurements of optical coherence tomography were evaluated according to causative genes using column scatter plots. Values for three common genes (*EYS*, *USH2A*, and *RHO*) were compared statistically.

Results: All patients with *PDE6B*, *PRPH2*, and *RPGR* mutations, those 55 years old or younger with *RP1L1* and *USH2A* mutations, and those 45 years old or younger with *EYS* and *RHO* mutations retained visual acuity of at least 0.1. All patients with *RPGR* mutations showed at least -20 dB mean deviation. Goldmann perimeter measures of 4/6 patients with *RHO* mutations showed remaining peripheral visual fields. Dark-adapted 0.01 and 3.0 ERGs were extinguished for most genes. Half of the patients with *RHO* RP maintained cone responses in light-adapted 3.0 and 3.0 flicker ERG. All patients with *PRPH2*, those 55 years old or younger with *USH2A* and *RP1L1*, and those 45 years old or younger with *PDE6B* and *EYS* mutations maintained subfoveal ellipsoid zones. No differences were identified between *EYS* and *USH2A* or *RHO* and *USH2A*.

Conclusions: Column scatter plots enabled comparisons of the associated severities and illustration of the ophthalmological measurements for every RP causative gene.

Translational Relevance: Analysis of mutations in specific genes may be helpful for determining visual prognoses in the clinical setting.

Introduction

Retinitis pigmentosa (RP) is a heterogeneous group of diseases caused by mutations in more than 50 genes.¹ Recent advances in genotype screening technology using next-generation sequencing have revealed the genetic background of RP in many cohorts.^{2–11} Ideally, this could lead to insights regarding the detailed clinical features of RP associated with each gene and has, for example, yielded descriptions of the phenotypes of mutation carriers and patients with RP themselves for one causative gene.^{12–14} However, to the best of our knowledge, only a single study has been published to date comparing the phenotypes of RP between all RP genes identified in a given cohort.¹⁵

A general treatment approach for RP is under development but has not yet been established. Therefore, the primary interest or concern of patients

generally is related to their own prognosis or to the likelihood of inheritance of the disorder by their children. Since retention of visual acuity is of particular relevance to the maintenance of their quality of life, it is desirable to obtain specific information regarding the visual prognosis associated with each causal gene.

Statistical methodologies for demonstrating significant differences represent the gold standard of scientific reports for comparing two groups consisting of large samples. However, comparisons of large numbers of groups or groups with smaller sample sizes weaken the statistical power for obtaining meaningful results. Thus, it might be inappropriate or impossible to compare differences in the features of RP, an orphan disease, among the numerous causative genes.

Huang et al.¹⁵ showed the relationship between visual acuity and specific causative genes using

column scatter plots in a cohort of patients with inherited retinal dystrophy from China. The Figure shown in the article illustrated disease duration from onset, visual acuity, and the affected genes in each individual. The advantages of this Figure were that the visual acuity of individuals was easy to understand owing to the use of color-coding, the severity of the RP associated with each gene was available, and we could determine the number of individuals associated with each causative gene, and, therefore, could consider that the genes associated with small numbers of patients were likely to include selection biases.

To obtain a similar level of detail for RP, this study aimed to describe the genotype–phenotype correlations in a cohort of Japanese patients with RP and to determine the efficacy of column scatter plots compared to traditional statistical methods for this purpose.

Methods

The current study adhered to the tenets of the Declaration of Helsinki. The institutional review board and ethics committee of Kyoto University Hospital approved the study protocols. All patients were fully informed regarding the details of this study, and written consent was obtained from each participant.

Participants

We reviewed retrospectively the clinical records of 121 patients with RP or Usher syndrome in the retinal degeneration service at Kyoto University Hospital who had been diagnosed molecularly in our previous study.⁷ Based on comprehensive ophthalmologic examinations and medical histories, patients exhibiting features of cone–rod dystrophy, macular dystrophy, Leber congenital amaurosis, or other specific named dystrophies had been excluded from the previous diagnostic study. The current cohort consisted solely of patients with RP or Usher syndrome with causative mutations in *EYS* ($n = 35$), *USH2A* ($n = 14$), *RHO* ($n = 7$), *RP1L1* ($n = 7$), *PDE6B* ($n = 6$), *RPGR* ($n = 5$), *PRPH2* ($n = 4$), *CNGA1* ($n = 3$), *CRX* ($n = 3$), *MAK* ($n = 3$), *MERTK* ($n = 3$), *PRPF31* ($n = 3$), *RP1* ($n = 3$), *SNRNP200* ($n = 3$), *C2orf71* ($n = 2$), *CNGB1* ($n = 2$), *GPR98* ($n = 2$), *RDH12* ($n = 2$), *RPE65* ($n = 2$), *TULP1* ($n = 2$), *BEST1* ($n = 1$), *IMPG2* ($n = 1$), *LRAT* ($n = 1$), *MYO7A* ($n = 1$),

NR2E3 ($n = 1$), *NRL* ($n = 1$), *PRCD* ($n = 1$), *PRPF6* ($n = 1$), *ROM1* ($n = 1$), and *TOPORS* ($n = 1$).

Column Scatter Plots

The column scatter plots were styled based on the graphs presented by Huang et al.¹⁵ The list of genes was arrayed across the x -axis, the right y -axis represented the percentage of plots with relatively good values, and the left y -axis showed the age at examination (although the original Figure adopted the duration from onset).¹⁵ The color of each point represented the categorized value for the respective measure obtained from ophthalmological examinations of the right eye.

Visual Acuity

Decimal visual acuity was measured using a Landolt chart. Visual acuity was divided into five categories ranging from normal (1.0 or better) through loss of vision (worse than 0.01) with each category indicated by a separate color as shown in Figure 1. The genes on the x -axis were arranged according to the percentage of patients with 0.1 or better visual acuity; this was shown using a line graph. For example, all patients (3/3) with *RPGR* mutations had 0.1 or better visual acuity, while one of three patients with *CRX* mutations had visual acuity worse than 0.1. Thus, the *RPGR* gene was positioned on the left of the *CRX* gene. Genes with the same percentage were arranged alphabetically. As a result, the genes arranged to the left of the x -axis were associated with more patients with good visual acuity than those to the right.

Central Visual Field

Patients underwent central visual field tests using a 10-2 SITA standard program with a Humphrey Field Analyzer (HFA; Carl Zeiss Meditec, Inc., Dublin, CA). Data sets with fixation loss scores of 20% or more or with false-positive or false-negative errors of 33% or more were discarded. Mean deviations (MDs) were categorized into four groups ranging from better than -10 through -30 dB or worse with each category indicated by a separate color, as shown in Figure 1. The genes on the x -axis were arranged according to the percentage of patients with better than -20 dB, which was shown using a line graph.

Peripheral Visual Field

Patients underwent visual field tests using the Goldmann perimeter (Haag Streit, Bern, Germany). The areas of V4e isopter were measured with Image J 1.48 software (National Institutes of Health, Bethes-

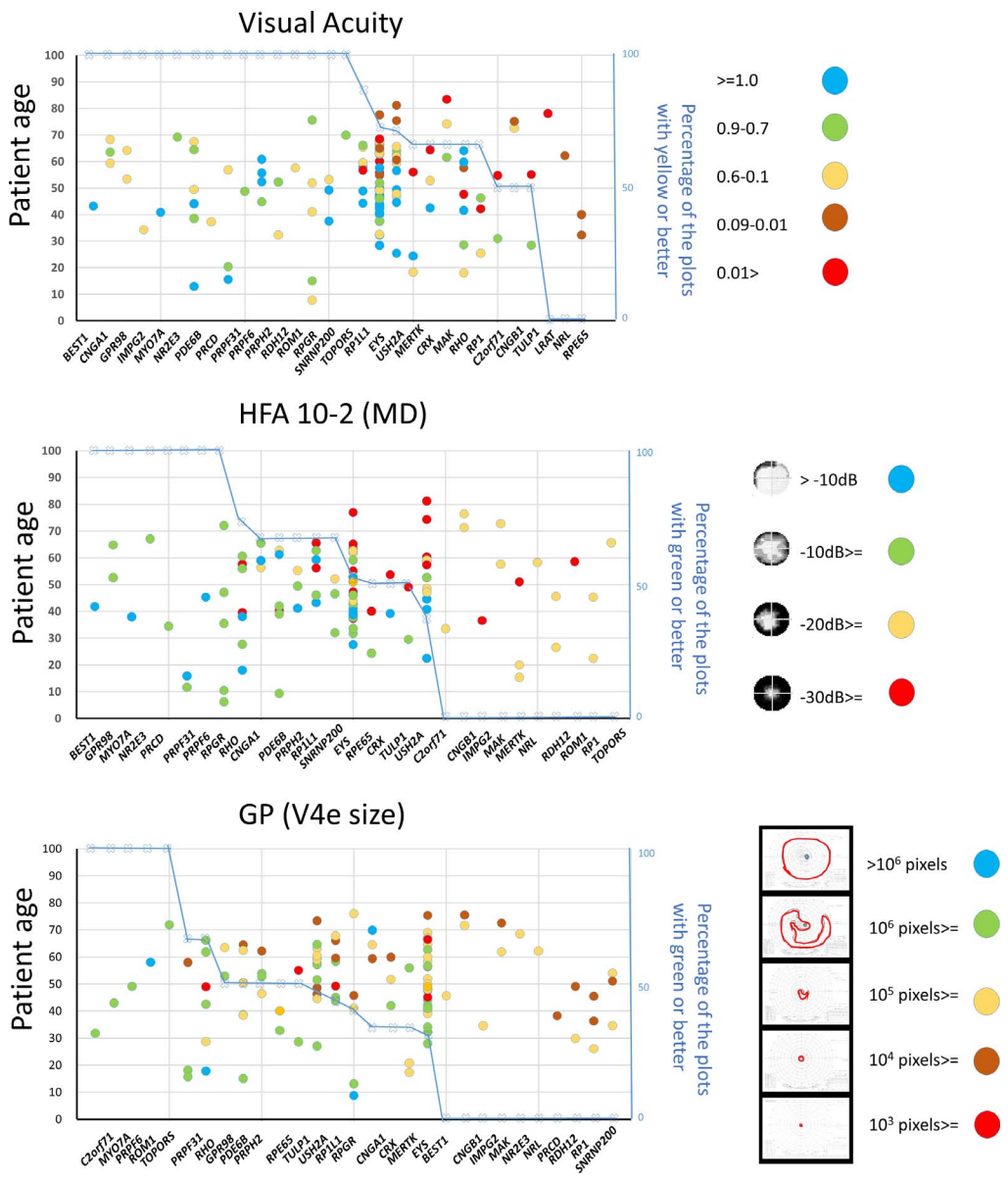


Figure 1. Column scatter plots of visual acuity, central visual field, and peripheral visual field arranged according to causative genes. Visual acuity is divided into five categories: normal (1.0 or better, *blue*), sufficient to obtain a driver’s license in Japan (0.9–0.7, *green*), able to distinguish letters (0.6–0.1, *yellow*), poor (0.09–0.01, *brown*), and loss of vision (worse than 0.01, *red*). The genes on the x-axis are arranged according to the percentage of associated RP cases with visual acuity 0.1 or better (*blue line*). The MD of the Humphrey Field Analyzer (HFA) 10-2 program is categorized into four groups as shown in the *legend*. The genes on the x-axis are arranged according to the percentage of associated RP cases with better than –20 dB (*blue line*). The areas of V4e isopter measured using the Goldmann perimeter are divided into five categories, as shown in the *legend*. The genes on the x-axis are arranged according to the percentage of associated RP cases with more than 10^5 pixels per visual field (*blue line*). The *left y-axis* shows the ages of the patients.

da, MD) as described previously.¹⁶ The whole image of the scanned result was equivalent to 2.1×10^6 pixels. The areas were divided into five categories ranging from $\geq 10^6$ to $\leq 10^3$ pixels with each category indicated by a separate color, as shown in **Figure 1**. Since most of the visual fields restricted concentrically within 10° resulted in 10^5 pixels or less, the genes on

the x-axis were arranged according to the percentage of patients with more than 10^5 pixels of visual field, shown using a line graph.

Electroretinography (ERG)

Electroretinography was performed according to the International Society for Clinical Electrophysiol-

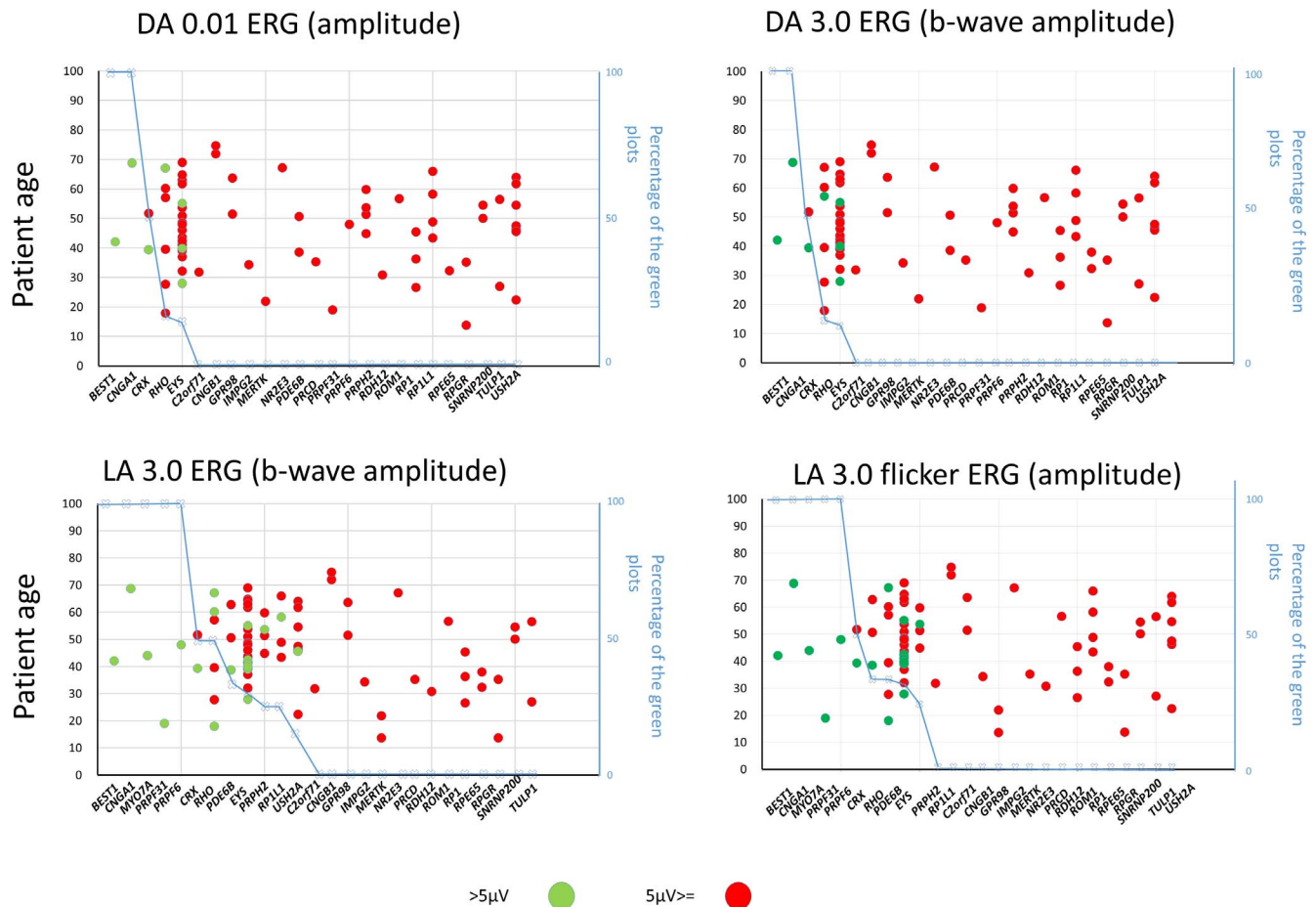


Figure 2. Column scatter plots of the amplitudes of ERG. The amplitudes in dark-adapted 0.01 ERG (DA 0.01 ERG) and light-adapted 3.0 flicker ERG (LA 3.0 flicker ERG) and of the b-wave in dark-adapted 3.0 ERG (DA 3.0 ERG) and light-adapted 3.0 ERG (LA 3.0 ERG) are divided into two categories: larger than $5 \mu\text{V}$ (green) and $5 \mu\text{V}$ or smaller (red). The genes on the x -axis are arranged according to the percentage of associated RP cases with larger than $5 \mu\text{V}$ of amplitude (blue line). The left y -axes show the ages of the patients.

ogy of Vision (ISCEV) standard protocol 2008 version using an LS-C200 stimulator (Mayo Co., Nagoya, Japan) and a Neuropack MEB-2204 signal processor (Nihon Kohden, Tokyo, Japan). The amplitudes in dark-adapted 0.01 ERG and light-adapted 3.0 flicker ERG, and the amplitudes of the b-wave in dark-adapted 3.0 ERG and light-adapted 3.0 ERG were divided into two groups (>5 and $\leq 5 \mu\text{V}$), with color-coding as shown in Figure 2. This was because waves of $5 \mu\text{V}$ or less were difficult to distinguish from noise in our recording condition. The genes on the x -axis were arranged according to the percentage of patients in the former group, shown using a line graph. Because amplitudes of more than $5 \mu\text{V}$ in dark-adapted 3.0 oscillatory potentials were recorded only in a patient with *EYS* mutations, the graph was omitted from Figure 2.

Cataracts

Patients were divided into three groups according to lens status, as determined based on clinical records, as follows: cataract (–), cataract (+), and intraocular lens (Fig. 3). Posterior or anterior subcapsule opacity or nucleus cataract with Emery-Little grade 3 or more was defined as cataract (+). The genes on the x -axis were arranged according to the percentage of patients in the cataract (–) group, shown using a line graph.

Optical Coherence Tomography (OCT)

We obtained 30° foveal cross scans (vertical and horizontal) using a Spectralis+ OCT system (Heidelberg Engineering, Heidelberg, Germany). The presence of cystoid macular edema (CME) and epiretinal membrane (ERM) were confirmed from cross scans by two authors (KO and SM). The genes on the x -axis were arranged according to the percentages of

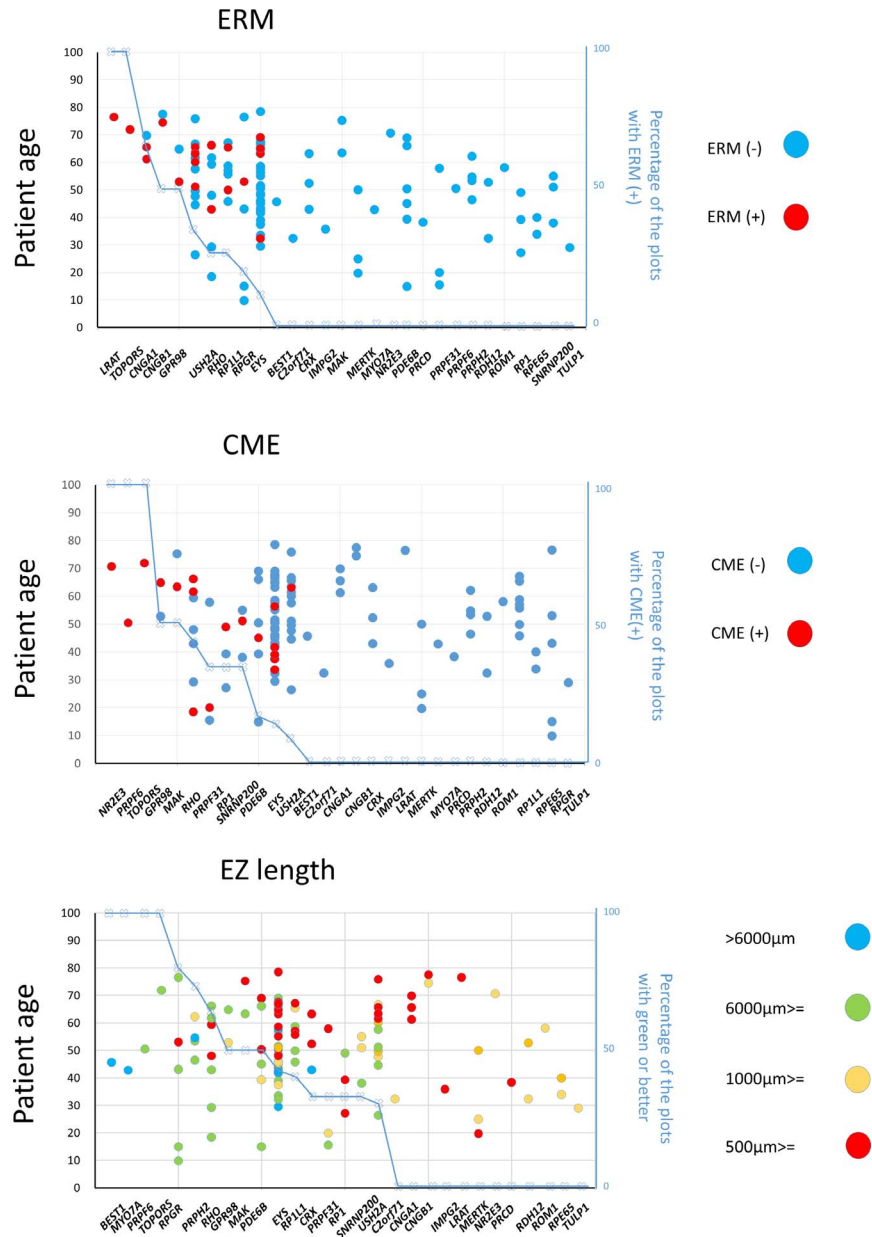


Figure 4. Column scatter plots of measurements of OCT. Patients with epiretinal membrane or cystoid macular edema are shown as *red plots*. The patients without ERM or CME are shown as *blue plots*. The genes on the x-axis are arranged according to the percentage of associated RP cases with ERM or CME. The averaged EZ length of the cross scans was divided into four categories: almost normal (more than 6000 μm , *blue*), within the macular area (6000 μm or less, *green*), within the foveal center field (1000 μm or less, *yellow*), and almost extinguished (500 μm or less, *red*). The genes on the x-axis are arranged according to the percentage of associated RP cases with more than 1000 μm of EZ (*blue line*). The *left y-axes* show the ages of the patients.

2). Although only a single patient with *RHO* mutation and three with *EYS* mutation showed rod response, more patients exhibited larger amplitude in light adapted 3.0 ERG or 3.0 flicker ERG. As a result, seven of 74 patients showed measurable peaks in dark-adapted 0.01 ERG and 3.0 ERG. Twenty of 77 patients and 20 of 75 showed measurable peaks in

light-adapted 3.0 ERG and 3.0 flicker ERG, respectively. Half of the patients with *RHO*-associated RP maintained the cone response.

Cataracts were observed generally in patients 40 years old or older (Fig. 3). Forty of 62 patients and 32 of 38 patients had cataracts or underwent cataract surgery at 50 years old or older and 60 years old or

Table 1. Comparison of RP Phenotypes Associated With the *EYS* and *USH2A* Genes

	<i>EYS</i> (n = 14)	Shapiro-Wilk Test	<i>USH2A</i> (n = 14)	Shapiro-Wilk Test	P Value ^a
Age	57.1 ± 11.8	P = 0.573	57.5 ± 12.7	P = 0.481	P = 0.604
Visual acuity	0.88 ± 1.2	P = 0.017	0.69 ± 0.88	P = 0.046	P = 0.701 ^b
GP, pixels	162,122 ± 266,168	P < 0.001	134,256 ± 234,754	P < 0.001	P = 0.929 ^b
HFA10-2 MD, dB	-19.3 ± 12.0	P = 0.232	-21.9 ± 10.2	P = 0.211	P = 0.559
Cataract or IOL	9/14		8/14		P = 1.000 ^c
ERM	2/14		5/14		P = 0.385 ^c
CME	0/14		1/14		P = 1.000 ^c
EZ length, μm	1724 ± 2627	P < 0.001	995 ± 1666	P = 0.001	P = 0.208 ^b
0.01 DA, μV	17.6 ± 35.1	P < 0.001	0.0	-	P = 0.391 ^b
3.0 DA, μV	15.6 ± 29.5	P < 0.001	0.0	-	P = 0.317 ^b
3.0 LA, μV	12.2 ± 19.4	P < 0.001	1.3 ± 3.3	P < 0.001	P = 0.256 ^b
3.0 LA flicker, μV	6.7 ± 12.4	P < 0.001	0.0	-	P = 0.180 ^b

GP, Goldmann perimeter; HFA10-2, Humphrey Field Analyzer 10-2 program; IOL, intraocular lens; 0.01 DA, dark-adapted 0.01 ERG; 3.0 DA, dark-adapted 3.0 ERG; 3.0 LA, light-adapted 3.0 ERG; 3.0 LA flicker; light-adapted 3.0 flicker ERG.

^a P values are according to paired *t*-test unless otherwise noted.

^b Wilcoxon signed rank test.

^c χ^2 test.

older, respectively. Less than half of the patients with *PRPH2*, *RPGR*, and *RHO* mutations had cataracts or underwent cataract surgery.

The epiretinal membrane was observed in elderly patients but was absent in those with *PDE6B* and *PRPH2* mutations (Fig. 4). Moreover, CME was observed even in younger patients compared to ERM, but no patients with *RPIL1* and *RPGR* mutations had CME (Fig. 4). All patients with *PRPH2* mutations, those 55 years old or younger with *USH2A* and *RPIL1* mutations, and those 45 years old or younger with *PDE6B* and *EYS* mutations maintained subfoveal EZ. In addition, four of five patients with *RPGR* mutations and five of seven patients with *RHO* mutations had EZ measures longer than 1000 μm.

Statistical Comparisons among *USH2A*, *EYS*, and *RHO*

Because of age matching, we were able to analyze comparisons between 14 patients with *EYS* mutations and 14 with *USH2A* mutations, and between six with *RHO* mutations and six with *USH2A* mutations.

The small sample size of each group did not yield normal distributions for visual acuity, Goldman perimetry, EZ length, or ERG parameters. Thus, Wilcoxon signed rank tests or paired *t*-tests were used, depending on the distribution. Table 1 shows the comparison between the representative AR-RP genes (*EYS* versus *USH2A*). There were no significant

differences observed for any parameters. Table 2 shows the comparison between the representative AD-RP and AR-RP genes (*RHO* versus *USH2A*). Although the visual fields measured using the Goldmann perimeter tended to be larger in *RHO*-associated RP than in *USH2A*-associated RP, the differences were not statistically significant.

Discussion

In this study, clinical measurements of Japanese patients with RP were shown according to each identified RP gene using column scatter plots. For genes mutated in a relatively large number of patients, such as *EYS*, we could estimate the associated age of decreasing quality of vision and thereby decreasing quality of life. Similar information for each gene would allow more objective and accurate consultations for individual patients than currently is available. However, the most common causal genes identified in Japanese patients with RP tended to be positioned toward the center of the *x*-axis. Thus, statistical analysis did not result in the identification of significant differences of clinical measurements between representative autosomal and recessive or recessive and dominant genes. Therefore, in terms of comparing the potential clinical outcome of each gene, our results suggested that many genes, especially those commonly mutated in RP, might overlap in

Table 2. Comparison of Retinitis Pigmentosa Phenotypes Associated With the *RHO* and *USH2A* Genes

	<i>RHO</i> , n = 6	Shapiro-Wilk Test	<i>USH2A</i> , n = 6	Shapiro-Wilk Test	P Value ^a
Age	48.2 ± 17.0	P = 0.289	49.5 ± 14.0	P = 0.425	P = 0.379
Visual acuity	0.67 ± 1.2	P = 0.003	0.17 ± 0.4	P < 0.001	P = 0.203 ^b
GP, pixels	409,862 ± 469,950	P = 0.219	210,242 ± 336,229	P = 0.018	P = 0.108 ^b
HFA10-2 MD, dB	-17.8 ± 11.7	P = 0.075	-17.7 ± 11.6	P = 0.790	P = 0.974
Cataract or IOL	2/6		2/6		P = 1.000 ^c
ERM	2/6		2/6		P = 1.000 ^c
CME	3/6		0/6		P = 0.182 ^c
EZ length, μm	1413 ± 1143	P = 0.152	1795 ± 1936	P = 0.187	P = 0.600
0.01 DA, μV	0.0	P < 0.001	0.0	-	P = 1.000 ^b
3.0 DA, μV	10.8 ± 24.2	P < 0.001	0.0	-	P = 1.000 ^b
3.0 LA, μV	9.5 ± 6.4	P = 0.190	0.0	-	P = 0.282
3.0 LA flicker, μV	7.4 ± 12.6	P = 0.013	0.0	-	P = 0.258 ^b

^a P values are according to paired *t*-test unless otherwise noted.

^b Wilcoxon signed rank test.

^c χ^2 test.

terms of their associated clinical course, as many clinicians have previously considered to be the case.

The visual acuity of patients with RP usually remains within the normal range, even in the advanced stage of the disease. Half of our patients (61/121) had good visual acuity, sufficient to obtain a driver's license, and approximately 75% of patients (94/121) had the minimum acuity necessary to read letters. Nonearly onset RP genes, such as *PDE6B*, *PRPH2*, *USH2A*, and *EYS*, showed 0.1 or better visual acuity at the age of 45 years or younger. These observations indicated that most Japanese patients with RP can continue their employment by selecting deskwork incorporating monitors or low vision aid devices by the age of 45. Notably, *RHO* and *RPGR*, which are considered to cause earlier onset RP than the formerly listed four genes, were associated with relatively good visual acuity, even in older patients. There is little information about *RP11*-associated RP, which was reported in the UK only relatively recently.¹⁷ However, according to our previous work, *RP11* accounts for 8.6% of AR-RP in Japan.⁷ The decline in visual acuity we had observed was similar to that observed with *USH2A* or *EYS* mutations. In comparison, the good visual acuity suggested by our results to be associated with the *BEST1* gene or the poor visual acuity suggested to be associated with the *RPE65* gene might be over- or underestimated because of the small sample size used in this study.

The HFA 10-2 program measures represent the central visual functioning of patients with RP, even at the advanced stage.¹⁸ In X-linked RP (such as that

caused by *RPGR* mutation), visual disturbances are thought to be more severe than in other forms of RP.¹⁹ Conversely, good visual acuity of *RPGR*-associated RP was found in our study, supported by an MD of more than -20 dB. However, this good central visual function might be caused by the sampling bias of our patients with the *RPGR* mutation. In this study, the five patients with *RPGR* mutations were male and the study did not include female carriers. However, only one patient had a mutation in ORF15, while 60% of disease-causing mutations have been shown to be located in this region.²⁰ The cohort in this study included patients diagnosed genetically by previous targeted exome sequencing, and the median coverage of the ORF15 was zero, which might explain the small number of patients shown to have ORF15 mutations. Indeed, the shortcomings of next-generation sequencing with respect to the sequencing of ORF15 in *RPGR* have been reported.²⁰

Cataracts are the common complication of RP. The scatter plots indicated that in most patients with RP cataracts develop before 60 years of age. All RP genes had similar tendencies. Because fewer than 16% of patients require cataract surgery before 65 years of age in the normal Japanese population,²¹ cataracts impair visual function earlier in patients with RP than in the general population.

The residual EZ is known to be associated strongly with visual acuity and to decline with disease progression.^{22,23} Phenotypic variety is common in dystrophies associated with *PRPH2*; however, all

patients diagnosed with RP with *PRPH2* mutation in this study had EZ measures of longer than 1000 μm . This is concordant with a recent report of patients with RP and *PRPH2* mutations from France.²⁴ On the other hand, *EYS* and *USH2A* were common AR-RP genes in Japan. The subfoveal EZ associated with mutation of these genes is likely to be retained through the fourth decade. This is very informative when considering public health or the support of Japanese patients with RP.

RP is complicated by CME and ERM. The higher prevalence of ERM in older patients with RP was consistent with that in the normal population. Interestingly, no patients with *PDE6B* and *PRPH2* had ERM. Moreover, to our knowledge, no previous reports have shown the absence of ERM in the context of *PDE6B* and *PRPH2*. Our previous study using spectral domain OCT estimated the prevalence of CME as 26.9% in a genotype-undetermined RP cohort.²⁵ The current results showed that 18 of 116 patients (15.5%) had CME, which was a lower percentage than that in a previous report, potentially because the previous report included both eyes and investigated volume scans instead of cross scans. CME occurred in younger patients than ERM; thus, CME may occur during an earlier stage of RP. Two older patients with CME with *RHO* mutation (66 and 62 years old) retained the cone response in ERG, suggesting a mild phenotype. This is consistent with our previous report showing that the CME was located predominantly in an area in which the external limiting membrane remained.²⁵ The absence of the CME in patients with *RPGR* and *RP1L1* mutations was interesting. The most plausible explanation for this observation was selection bias due to the small sample size. Birch et al.²⁶ did not refer to CME in their OCT study in a cohort with *RPGR*-RP.

In our cohort, patients with RP and *RHO* mutations had relatively large visual fields. This also is consistent with a previous report in French patients with RP.²⁷ Sandberg et al.²⁸ demonstrated that the severity of the disease was correlated with the location of the amino acid residue altered by the mutation, and showed that the decline in the visual field was mild for patients carrying gene mutations at the transmembrane domain. However, the four patients with a preserved visual field in our study carried mutations in other domains. Therefore, more cases are needed to allow a detailed discussion of the effects of each mutation.

We often see patients with RP with moderately preserved ERG in the clinical setting. These patients

include young patients and those with sectorial RP. In this study, however, only one of 10 and one of four patients showed measurable peaks in rod and cone responses, respectively. The patients with preserved responses were not limited to youth but rather showed mutations in specific genes, such as *EYS* or *RHO*. These findings suggested that electrophysiological findings might be more effective for identification of causative genes than other ophthalmologic measures.

Statistical analysis is the gold standard of scientific reports for comparing two groups consisting of large samples. However, not more than 35 patients had even the most commonly mutated RP gene within our cohort. As a result, we presented the results of paired *t*-tests using 14 and six sample sets. The small sample groups did not show normal distributions in some measurements, requiring us to use the Wilcoxon signed rank test. Accordingly, we did not identify any significant differences between the parameters associated with mutations in *EYS* and *USH2A* or between the parameters associated with mutations in *RHO* and *USH2A*. Although the phenotypes associated with these genes might, indeed, overlap, we recommend that these results be treated with caution because of the lack of statistical power owing to the small sample sizes. The formation of a consortium would be the key to overcoming this problem. It is relatively straightforward to obtain standardized information regarding genomics or visual acuity between institutions, and it is possible to compare these findings. However, ERG and the Goldmann perimeter still show variable results between hospitals, even if obtained using standardized protocols. These difficulties might result in the performance of few genotype–phenotype correlation studies of RP using statistical methods.^{29–32}

One limitation of this study is that our scatter plots were integrated based not on specific mutations but on mutated genes. The type of mutation (nonsense, missense, insertion, deletion, or copy number variation) and the location of the mutation (splice site, intron, exon, or protein domain) within a gene are thought to influence the RP phenotype. The mixture of these mutations in this study possibly confused the determination of genotype–phenotype correlations. However, the scatter plots could be applied to mutation-based analysis if additional numbers of patients with RP are diagnosed molecularly in a large consortium.

In conclusion, the use of column scatter plots enabled the comparison of the severity associated with RP genes and the visualization of the ophthal-

mological measurements of RP for every gene. This could not be achieved currently by statistical approaches because of the large number of causative genes. The results suggest that the phenotypes of the common causative genes in Japan might overlap in the standard clinical course; however, the prognosis of visual function based on the known outcomes associated with each causative gene would be helpful for daily consultations. Another advantage of the scatter plot is that we can add points or even plots for each new patient, which would result in more accurate collective information. Thus, the column scatter plots might be an effective tool for managing the clinical course of RP based on causative genes.

Acknowledgments

Supported by The Japan Society for the Promotion of Science (JSPS), Tokyo, Japan (Grant-in-Aid for Scientific Research, no. 26861445).

Disclosure: **K. Ogino**, None; **A. Oishi**, None; **M. Oishi**, None; **N. Gotoh**, None; **S. Morooka**, None; **M. Sugahara**, None; **T. Hasegawa**, None; **M. Miyata**, None; **N. Yoshimura**, None.

References

- Hartong DT, Berson EL, Dryja TP. Retinitis pigmentosa. *Lancet*. 2006;368:1795–1809.
- Bowne SJ, Sullivan LS, Koboldt DC, et al. Identification of disease-causing mutations in autosomal dominant retinitis pigmentosa (adRP) using next-generation DNA sequencing. *Invest Ophthalmol Vis Sci*. 2011;52:494–503.
- Daiger SP, Bowne SJ, Sullivan LS, et al. Application of next-generation sequencing to identify genes and mutations causing autosomal dominant retinitis pigmentosa (adRP). *Adv Exp Med Biol*. 2014;801:123–129.
- Fernandez-San Jose P, Corton M, Blanco-Kelly F, et al. Targeted next-generation sequencing improves the diagnosis of autosomal dominant retinitis pigmentosa in Spanish patients. *Invest Ophthalmol Vis Sci*. 2015;56:2173–2182.
- Fu Q, Wang F, Wang H, et al. Next-generation sequencing-based molecular diagnosis of a Chinese patient cohort with autosomal recessive retinitis pigmentosa. *Invest Ophthalmol Vis Sci*. 2013;54:4158–4166.
- Neveling K, Collin RW, Gilissen C, et al. Next-generation genetic testing for retinitis pigmentosa. *Hum Mutat*. 2012;33:963–972.
- Oishi M, Oishi A, Gotoh N, et al. Comprehensive molecular diagnosis of a large cohort of Japanese retinitis pigmentosa and Usher syndrome patients by next-generation sequencing. *Invest Ophthalmol Vis Sci*. 2014;55:7369–7375.
- Simpson DA, Clark GR, Alexander S, Silvestri G, Willoughby CE. Molecular diagnosis for heterogeneous genetic diseases with targeted high-throughput DNA sequencing applied to retinitis pigmentosa. *J Med Genet*. 2011;48:145–151.
- Wang F, Wang H, Tuan HF, et al. Next generation sequencing-based molecular diagnosis of retinitis pigmentosa: identification of a novel genotype–phenotype correlation and clinical refinements. *Hum Genet*. 2014;133:331–345.
- Wang X, Wang H, Sun V, et al. Comprehensive molecular diagnosis of 179 Leber congenital amaurosis and juvenile retinitis pigmentosa patients by targeted next generation sequencing. *J Med Genet*. 2013;50:674–688.
- Zhao L, Wang F, Wang H, et al. Next-generation sequencing-based molecular diagnosis of 82 retinitis pigmentosa probands from Northern Ireland. *Hum Genet*. 2015;134:217–230.
- Aguirre GD, Yashar BM, John SK, et al. Retinal histopathology of an XLRP carrier with a mutation in the RPGR exon ORF15. *Exp Eye Res*. 2002;75:431–443.
- Comander J, Weigel-DiFranco C, Sandberg MA, Berson EL. Visual function in carriers of X-linked retinitis pigmentosa. *Ophthalmology*. 2015;122:1899–1906.
- Souied E, Segues B, Ghazi I, et al. Severe manifestations in carrier females in X linked retinitis pigmentosa. *J Med Genet*. 1997;34:793–797.
- Huang XF, Huang F, Wu KC, et al. Genotype–phenotype correlation and mutation spectrum in a large cohort of patients with inherited retinal dystrophy revealed by next-generation sequencing. *Genet Med*. 2015;17:271–278.
- Oishi A, Ogino K, Makiyama Y, Nakagawa S, Kurimoto M, Yoshimura N. Wide-field fundus autofluorescence imaging of retinitis pigmentosa. *Ophthalmology*. 2013;120:1827–1834.
- Davidson AE, Sergouniotis PI, Mackay DS, et al. RP1L1 variants are associated with a spectrum of inherited retinal diseases including retinitis pigmentosa and occult macular dystrophy. *Hum Mutat*. 2013;34:506–514.

18. Hirakawa H, Iijima H, Gohdo T, Imai M, Tsukahara S. Progression of defects in the central 10-degree visual field of patients with retinitis pigmentosa and choroideremia. *Am J Ophthalmol*. 1999;127:436–442.
19. Sandberg MA, Weigel-DiFranco C, Rosner B, Berson EL. The relationship between visual field size and electroretinogram amplitude in retinitis pigmentosa. *Invest Ophthalmol Vis Sci*. 1996;37:1693–1698.
20. Huang XF, Wu J, Lv JN, Zhang X, Jin ZB. Identification of false-negative mutations missed by next-generation sequencing in retinitis pigmentosa patients: a complementary approach to clinical genetic diagnostic testing. *Genet Med*. 2015;17:307–311.
21. Ministry of Health, Labour and Welfare. National Medical Care Expenditure Estimates FY2009 Statistics and Information Department. Minister's Secretariat, Ministry of Health, Labour and Welfare 2011.
22. Hood DC, Ramachandran R, Holopigian K, Lazow M, Birch DG, Greenstein VC. Method for deriving visual field boundaries from OCT scans of patients with retinitis pigmentosa. *Biomed Opt Express*. 2011;2:1106–1114.
23. Sandberg MA, Brockhurst RJ, Gaudio AR, Berson EL. The association between visual acuity and central retinal thickness in retinitis pigmentosa. *Invest Ophthalmol Vis Sci*. 2005;46:3349–3354.
24. Manes G, Guillaumie T, Vos WL, et al. High prevalence of PRPH2 in autosomal dominant retinitis pigmentosa in France and characterization of biochemical and clinical features. *Am J Ophthalmol*. 2015;159:302–314.
25. Makiyama Y, Oishi A, Otani A, et al. Prevalence and spatial distribution of cystoid spaces in retinitis pigmentosa: investigation with spectral domain optical coherence tomography. *Retina*. 2014;34:981–988.
26. Birch DG, Locke KG, Felius J, et al. Rates of decline in regions of the visual field defined by frequency-domain optical coherence tomography in patients with RPGR-mediated X-linked retinitis pigmentosa. *Ophthalmology*. 2015;122:833–839.
27. Audo I, Manes G, Mohand-Said S, et al. Spectrum of rhodopsin mutations in French autosomal dominant rod-cone dystrophy patients. *Invest Ophthalmol Vis Sci*. 2010;51:3687–3700.
28. Sandberg MA, Weigel-DiFranco C, Dryja TP, Berson EL. Clinical expression correlates with location of rhodopsin mutation in dominant retinitis pigmentosa. *Invest Ophthalmol Vis Sci*. 1995;36:1934–1942.
29. Ahn SJ, Cho SI, Ahn J, Park SS, Park KH, Woo SJ. Clinical and genetic characteristics of Korean occult macular dystrophy patients. *Invest Ophthalmol Vis Sci*. 2013;54:4856–4863.
30. Fernandez-San Jose P, Blanco-Kelly F, Corton M, et al. Prevalence of rhodopsin mutations in autosomal dominant retinitis pigmentosa in Spain: clinical and analytical review in 200 families. *Acta Ophthalmol*. 2015;93:e38–e44.
31. Ma L, Sheng XL, Li HP, et al. Identification of a novel p.R1443W mutation in RP1 gene associated with retinitis pigmentosa sine pigmento. *Int J Ophthalmol*. 2013;6:430–435.
32. Oh KT, Oh DM, Weleber RG, et al. Genotype-phenotype correlation in a family with Arg135Leu rhodopsin retinitis pigmentosa. *Br J Ophthalmol*. 2004;88:1533–1537.